^{22}Na$(n,p)^{22}$Ne and ^{22}Na$(n,\alpha)^{19}$F cross sections from 25 meV to 35 keV

P. E. Koehler and H. A. O'Brien
Physics Division, Los Alamos National Laboratory, Los Alamos, New Mexico 87545
(Received 23 May 1988)

The ^{22}Na(n,p_0), (n,p_1), (n,α_0), (n,α_1), and (n,α_2) cross sections have been measured at thermal neutron energy. In addition, the p_0 and p_1 cross sections have been measured from thermal energy to 420 eV and 35 keV, respectively. These new data were used to discern the structure of ^{23}Na near the neutron threshold. In particular, it was found that a $(\frac{7}{2})^+$ resonance dominates the p_1 cross section but contributes very little to the p_0 cross section. The p_0, and also most probably the (n,α_0) cross sections, are instead dominated by a separate $(\frac{5}{2})^+$ resonance. The ^{22}Na$(n,p)^{22}$Ne astrophysical reaction rate, $N_A\langle\sigma v\rangle$, was calculated using our new data and compared to published theoretical rates used in previous nucleosynthesis calculations. It was found that the theoretical rates are approximately a factor of 5 to 10 different from the experimental one at most temperatures measured. We discuss the possible implications of this difference on nucleosynthesis calculations for ^{22}Na and ^{22}Ne.

I. INTRODUCTION

The ^{22}Na$(n,p)^{22}$Ne and ^{22}Na$(n,\alpha)^{19}$F cross sections are of interest to both basic nuclear physics and nuclear astrophysics. In nuclear physics these reactions can play an important role in understanding the structure of ^{23}Na, especially near the ^{22}Na + n threshold. For example, although there have been reported measurements of the ^{22}Na$(n,p_0)^{22}$Ne and ^{22}Na$(n,p_1)^{22}$Ne cross sections at thermal energy,[1,2] the ^{22}Na$(n,p_1)^{22}$Ne cross section to 370 eV (Ref. 3) and ^{19}F$(\alpha,p)^{22}$Ne (Refs. 4 and 5) as well as ^{22}Ne$(p,p_1\gamma)^{22}$Ne (Ref. 5) measurements near the neutron threshold, the levels in ^{23}Na in this excitation region are not well understood. One motivation of this work was to make more extensive ^{22}Na + n measurements to aid in clarifying the structure of ^{23}Na at these energies.

In nuclear astrophysics, the ^{22}Na$(n,p)^{22}$Ne reactions may play a role in the nucleosynthesis of ^{22}Na and/or ^{22}Ne. The nucleosynthesis of these particular isotopes is of current interest because the origin of the neon-E anomaly[6] is not well understood and because of the possibility of observing ^{22}Na from extraterrestrial sources with gamma-ray telescopes.[7] For those calculations involving environments where the neutron flux is significant,[8–12] the ^{22}Na$(n,p)^{22}$Ne reaction may play the dominant role in the destruction of ^{22}Na. The astrophysical reactions rates[13,14] for this reaction that were used in previous calculations are based on theory. Because Hauser-Feshbach theory was used to calculate the cross section on which the reaction rate is based, it is not unreasonable to expect that the theoretical rate could be wrong by a significant amount for a nucleus as light as ^{23}Na. In fact, the theoretical rates[13,14] used in previous nucleosynthesis calculations, when extrapolated to low energies and converted to cross sections, are at least a factor of 10 smaller than previous measurements.[1–3] Hence, a second motivation for this work was to make measurements of the ^{22}Na$(n,p)^{22}$Ne cross sections to as high an energy as possible to allow an experimental determination of the astrophysical reaction rate.

II. EXPERIMENTAL PROCEDURES

The experimental technique used in these measurements has been published elsewhere,[15] so only the salient features will be presented here. The measurements were performed at the Los Alamos National Laboratory. The absolute cross sections at thermal neutron energy were measured at the Omega West Reactor (OWR). The remainder of the measurements were made at the Los Alamos Neutron Scattering Center (LANSCE).

The ^{22}Na for the samples was produced in an ultrapure aluminum target that was bombarded with a high-intensity beam of 800-MeV protons at the Los Alamos Meson Physics Facility (LAMPF). Chemical separation and purification of the ^{22}Na were performed by scientists at Dupont's Diagnostic Imaging Division (formerly New England Nuclear) utilizing special procedures and materials to minimize introduction of stable sodium and to eliminate contaminants.[16] The ^{22}Na was purchased from Dupont as sodium chloride in water. The samples were made by depositing the water solution into a shallow dimple in a 8.5-μm thick aluminum foil. A heat lamp shining on the sample served to speed up the evaporation of the water. The resulting deposits were fairly uniform and approximately 3 mm in diameter.

The protons and alpha particles were detected with silicon surface-barrier detectors. For most of the experiments, a single detector, 150-μm thick by 50 mm^2 in area, was used. In addition, separate LANSCE and OWR measurements were made with a ΔE-E detector telescope in order to reduce the background at higher neutron energies and lower pulse heights. The ΔE and E detectors were 10- and 150-μm thick, respectively. Both detectors had an area of 50 mm^2.

Measurements were made with two different samples.

The first OWR data and all of the LANSCE data were taken with a sample having a specific activity of 544 mCi/mg and containing 350 ng of ^{22}Na at the start of the measurements in March, 1987. The combination of this sample being too thick and the intense pileup from the decay products of the ^{22}Na caused the resolution to be degraded so much that it was not possible to resolve the various peaks from the ^{22}Na$(n,\alpha)^{19}$F reactions from one another and from the tail of the p_1 peak. A second, much thinner sample was made in January of 1988 from a solution of much higher specific activity (1200 mCi/mg) and contained about 75 ng of ^{22}Na. This sample was thin enough and of low enough activity to allow the alpha peaks to be almost completely resolved from one another and was used for later measurements of the thermal cross sections at the OWR. A typical pulse-height spectrum from the OWR measurements is shown in Fig. 1. The thinner sample was obtained too late to allow it to be used for the LANSCE measurements.

There is the possibility of an uncertainty in the α_2, and to a lesser extent, the α_1 cross sections, due to a possible ^{10}B contamination in the sample. The α_1 group from the ^{10}B$(n,\alpha_1)^7$Li*(0.48 MeV) ($\approx$90% of the thermal cross section) has almost the same energy as the α_2 group from the ^{22}Na$(n,\alpha)^{19}$F reactions. A limit on the size of a possible ^{10}B contamination was ascertained by searching for the α_0 and ^{7}Li$_1$ groups from the ^{10}B + n reactions. Because the ^{7}Li$_1$ group is fairly low in energy, it was necessary to use a relatively thin (e.g., the 10-μm-thick ΔE detector of the ΔE-E detector telescope mentioned above) detector to reduce the low-energy background during the search for this group. A benefit of using this detector was that the background in the region of the ^{22}Na$(n,\alpha)^{19}$F peaks was reduced considerably compared to the results obtained with the 150-μm thick detector. This helped to reduce the uncertainty in the measured cross sections for these groups. A pulse-height spectrum from the measurements taken with the 10-μm thick detector is shown in Fig. 2. No ^{10}B contamination was observed in these measurements. The results obtained with the 10-μm-thick detector indicate that there are less than 0.002 ^{10}B nuclei and 0.07 ^{6}Li nuclei per ^{22}Na nucleus in our sample. The ^{10}B and ^{6}Li contaminations in our sample are a factor of at least 250 and 3.6 times less, respectively, than in the sample used in Ref. 2, which had the lowest level of these contaminants of previous reported measurements.[1-3] It was determined that the maximum amount the α_1 group, from a possible ^{10}B contamination, could contribute to the ^{22}Na$(n,\alpha_2)^{19}$F cross section was less than 4%.

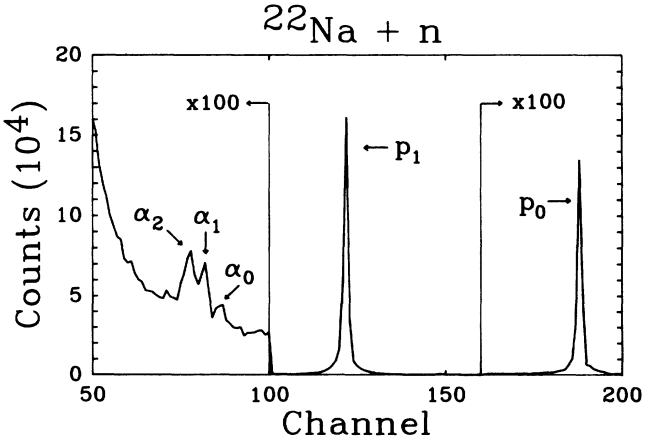

FIG. 1. A pulse-height spectrum obtained during the OWR measurements using a 150-μm-thick detector and the sample containing 75 ng of ^{22}Na. The peaks from the ^{22}Na + n reactions are labeled according to the outgoing reaction product.

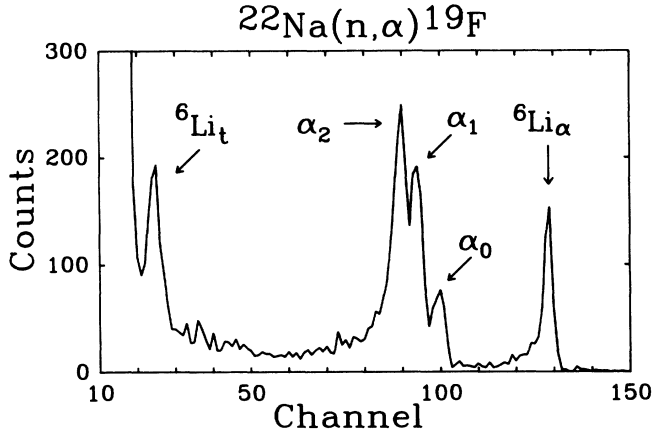

FIG. 2. A pulse-height spectrum obtained during the OWR measurements with a 10-μm-thick detector and the sample containing 75 ng of ^{22}Na. The peaks from the ^{22}Na$(n,\alpha)^{19}$F reactions are labeled according to the outgoing reaction product. In addition, the two peaks labeled ^{6}Li$_\alpha$ and ^{6}Li$_t$ are from the ^{6}Li$(n,\alpha)t$ reaction due to a ^{6}Li impurity in the sample.

Because the α peaks were not completely resolved from one another, even for the measurements made with the thinner sample, they were fit to skewed Gaussian shapes, including a smooth background, to obtain the yields for each group separately. The peak shape was determined by fitting the well-resolved α peak from the ^{6}Li$(n,\alpha)t$ reaction recorded in the 10-μm-thick detector. The errors in the individual α_0, α_1, and α_2 cross sections are dominated by the uncertainty involved in this fitting procedure, while the sum of the α_0–α_2 cross sections does not have this additional error.

The absolute thermal cross sections were measured at the OWR using gold-foil activation to determine the neutron flux, a calibrated ^{241}Am source to determine the detector solid angle, and a calibrated germanium detector to ascertain the number of ^{22}Na nuclei in the samples. The LANSCE data were measured relative to ^{6}Li$(n,\alpha)t$ and were converted from yields to cross sections using the known ^{6}Li$(n,\alpha)t$ cross sections,[17] and the absolute thermal cross sections for ^{22}Na we measured at the OWR. The details of this normalization, as well as the collimation, the data-acquisition techniques, the neutron energy resolution, and the small corrections to the data due to the anisotropy of the ^{6}Li$(n,\alpha)t$ cross section have been published elsewhere.[15]

III. RESULTS AND COMPARISON WITH OTHER MEASUREMENTS

The thermal cross sections we measured at the OWR are compared to previous results in Table I. The errors in the cross sections we report include both the statistical errors and estimates of the systematic uncertainties. The value we measured for the sum of the ^{22}Na(n,p_0), (n,p_1), (n,α_0), (n,α_1), and (n,α_2) thermal cross sections is substantially less than the total destruction cross section reported in Refs. 18 and 19 but is in good agreement with the value reported in Ref. 20. Our measurement of the p_0 thermal cross section is significantly larger than previous results.[2,3] All of these direct measurements are about a factor of 40 larger than this same cross section measured using the inverse reaction.[5] The value we measured for the p_1 thermal cross section is in agreement with the previous measurement of Ref. 1, but is just outside the error reported in Ref. 3 for the measurement of this cross section in Ref. 2. Our direct measurement of the α_0 thermal cross section is 30 times larger than the value given in Ref. 5 which was measured using the inverse reaction. There have been no other published reports of a direct measurement of the α_0 cross section. Our results do agree with the limits given in Refs. 1 and 3. Alternately, the value we measured for the ratio of the sum of the α_0–α_2 cross section to the (n,p) cross section is larger than the limit given in Ref. 2.

The results of our LANSCE measurements of the p_0 and p_1 cross sections are shown in Figs. 3 and 4, respectively. Due to the relatively small size of the p_0 cross section, in order to obtain sufficient statistics, the p_0 data were binned much more coarsely in neutron energy than was necessary for the p_1 data. Also, as a result of the relatively small size of the p_0 cross section, and the rapid decrease with energy of both the cross section and the neutron flux from the LANSCE, it was not possible to measure p_0 cross sections above 420 eV.

The only published measurements of the ^{22}Na$(n,p)^{22}$Ne or ^{22}Na$(n,\alpha)^{19}$F cross sections at other than thermal energy are the p_1 results of Ref. 3 to $E_n = 370$ eV, and the limit, $\sigma_{p1} < 11b$ at $E_n = 2$ keV, given in Ref. 2. Our measurements agree with this limit. Also, as can be seen in Fig. 4 our measurements are in fair agreement with those of Ref. 3. Both sets of data show that the p_1 cross section is dominated by a single resonance near 170 eV. The dashed curve in Fig. 4 shows the result of fitting our p_1 data using the single-level, Breit-Wigner formula. Assuming $J^\pi = \frac{7}{2}^+$ for this resonance, we obtain $E_0 = 178$ eV, $\Gamma_n^0 = 2.7$ eV, and $\Gamma_{p1} = 148$ eV. The dashed curve in Fig. 3 shows the expected contribution to the p_0 cross section from this $\frac{7}{2}^+$ resonance if it was responsible for the thermal p_0 cross section. It is obvious that this resonance contributes very little to the p_0 cross section.

In the preceding we have assumed that the J^π of the p_1 resonance is $\frac{7}{2}^+$, although it is possible to excite both $\frac{5}{2}^+$ and $\frac{7}{2}^+$ levels in ^{23}Na from s-wave neutron interactions with ^{22}Na $(I^\pi = 3^+)$. Although equally good fits to the p_1 resonance can be obtained using either J^π, penetrability considerations favor a $\frac{7}{2}^+$ assignment over a $\frac{5}{2}^+$. The fact that the p_1 resonance does not contribute much to the p_0 channel indicates that the width of the resonance

TABLE I. ^{22}Na + n measurements at thermal energy.

Quantity measured	Result	Reference
Total destruction	$(90\pm10)\times10^3 b$	18
Total destruction	$(35.9\pm1.2)\times10^3 b$	19
Total destruction	$(28.3\pm0.6)\times10^3 b$	20
$\sigma_{p0}+\sigma_{p1}+\sigma_{\alpha0}+\sigma_{\alpha1}+\sigma_{\alpha2}$	$(28.1\pm2.4)\times10^3 b$	Present work
σ_{p1}	$(4\pm2)\times10^4 b$	1
$\sigma_{p0}+\sigma_{p1}$	$(30.6\pm2.6)\times10^3 b$[a]	2,3
σ_{p1}	$(27.6\pm2.4)\times10^3 b$	Present work
σ_{p0}/σ_{p1}	$(7.4\pm0.2)\times10^{-3}$	2
σ_{p0}/σ_{p1}	$(6\pm2)\times10^{-3}$	3
σ_{p0} (reciprocity)	$5.6b$	5
σ_{p0}/σ_{p1}	$(8.5\pm0.5)\times10^{-3}$	Present work
$\sigma_{\alpha0}/\sigma_{p1}$	$(1\pm1.5)\times10^{-3}$	1
$\sigma_{\alpha0}/\sigma_{p1}$	$\ll 1$	3
$\sigma_{\alpha0}$ (reciprocity)	$1.2b$	5
$\sigma_{\alpha0}/\sigma_{p1}$	$(1.3\pm0.3)\times10^{-3}$	Present work
$\sigma_{\alpha1}/\sigma_{p1}$	$(3.4\pm0.8)\times10^{-3}$	Present work
$\sigma_{\alpha2}/\sigma_{p1}$	$(4.6\pm1.2)\times10^{-3}$	Present work
$(\sigma_{\alpha0}+\sigma_{\alpha1}+\sigma_{\alpha2})/(\sigma_{p0}+\sigma_{p1})$	$<\frac{1}{500}$	2
$(\sigma_{\alpha0}+\sigma_{\alpha1}+\sigma_{\alpha2})/(\sigma_{p0}+\sigma_{p1})$	$(9.4\pm1.4)\times10^{-3}$	Present work

[a]Statistical error is given in Ref. 2 as $\pm0.6\times10^3$. Error listed is from quote of Ref. 2 in Ref. 3.

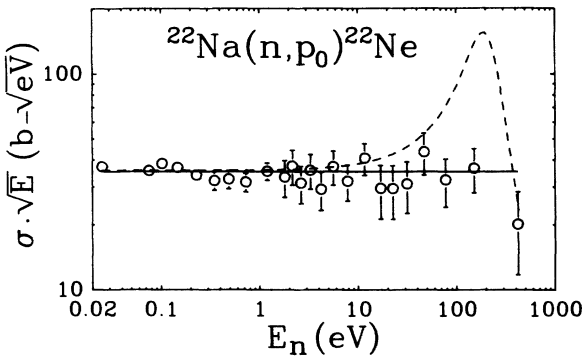

FIG. 3. The reduced cross section for the ^{22}Na$(n,p_0)^{22}$Ne reaction vs laboratory neutron energy. The circles are the results of our LANSCE measurements. The dashed curve shows the expected cross section if the $\frac{7}{2}^+$, p_1 resonance was responsible for the p_0 thermal cross section. The solid curve shows the result of fitting the data to a strict $1/v$ shape.

is very small in the p_0 channel. The ratio of the proton penetrabilities for the decay from a $\frac{5}{2}^+$ level in ^{23}Na to the ground and first-excited states of ^{22}Ne is $P_{p0}(l=2)/P_{p1}(l=0)=0.4$, while for a $\frac{7}{2}^+$ level the ratio is $P_{p0}(l=4)/P_{p1}(l=2)=0.04$. Because a $\frac{7}{2}^+$ assignment gives a smaller value for this ratio (and therefore most probably a smaller ratio of the widths), it is favored over a $\frac{5}{2}^+$. The above penetrability arguments, together with the lack of obvious interference effects in the cross sections, favor a $\frac{5}{2}^+$ assignment for the resonance responsible for the p_0 cross section. This same $\frac{5}{2}^+$ level may also be responsible for much of the p_1 cross section at energies above where the $\frac{7}{2}^+$ gives a good fit to the p_1 data. The

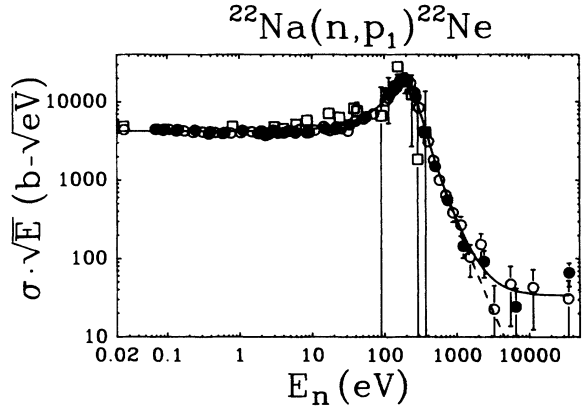

FIG. 4. The reduced cross section for the ^{22}Na$(n,p_1)^{22}$Ne* (1.27 MeV) reaction vs laboratory neutron energy. The solid and open circles are the results of our LANSCE measurements with a single detector and a ΔE-E detector telescope, respectively. For clarity, only every fifth data point is shown for energies below 100 eV. The data of Ref. 3 are shown for comparison as open squares. The dashed curve is the result of fitting our data to a single $\frac{7}{2}^+$ resonance. The solid curve results from fitting our data to the sum of a $\frac{7}{2}^+$ resonance and a noninterfering (e.g., $\frac{5}{2}^+$) resonance having a strict $1/v$ shape.

solid curve in Fig. 3 shows the result of fitting the p_0 cross section to a strict $1/v$ shape. The solid curve in Fig. 4 shows the result of fitting the p_1 cross section to the sum of the $\frac{7}{2}^+$ resonance discussed above and a noninterfering (e.g., $\frac{5}{2}^+$) resonance with a strict $1/v$ shape. Both fits agree well with the data. Assuming a single broad $\frac{5}{2}^+$ level in ^{23}Na is responsible for these $1/v$ contributions to the p_0 and p_1 cross sections, we obtain $\Gamma_{p0}/\Gamma_{p1}=1.0$. It is not possible to determine much else about this possible $\frac{5}{2}^+$ resonance except that it must be fairly broad and is most probably located below threshold.

IV. STRUCTURE OF ^{23}Na NEAR THE NEUTRON THRESHOLD

Our data indicate that at least two levels in ^{23}Na near the neutron threshold are needed to explain the ^{22}Na(n,p_0) and (n,p_1) cross sections. The parameters we obtained from the analysis of our data are compared to previous work in Table II. The three parameters, E_0, Γ_n^0, and Γ_{p1} we obtain from fitting our p_1 data to a $\frac{7}{2}^+$ resonance are in fair agreement with those obtained in Ref. 3. From penetrability arguments we have tentatively concluded that a $J^\pi=\frac{7}{2}^+$ assignment is favored for the p_1 resonance and that the p_0 resonance probably has $J^\pi=\frac{5}{2}^+$. The results of cluster-model calculations[2] further strengthen these J^π assignments. The model calculations indicate that for $J^\pi=\frac{5}{2}^+$ the ratio of the mean partial widths should be $\Gamma_{p0}/\Gamma_{p1}\approx 0.4$, while for $J^\pi=\frac{7}{2}^+$ the ratio is $\Gamma_{p0}/\Gamma_{p1}<1.3\times10^{-3}$. These numbers are in agreement with our observations if $J^\pi=\frac{7}{2}^+$ is assumed for the p_1 resonance. However, the conclusion drawn in Ref. 2 that the $\frac{7}{2}^+$ p_1 resonance has been observed in ^{19}F$(\alpha,p)^{22}$Ne measurements[4] is not supported by our measurements, nor by previous ^{22}Na$(n,p)^{22}$Ne data.[1,3]

Because previous measurements of the p_0 cross section had been made at thermal energy only, it was assumed[2,3] that the same resonance is being observed in both the p_0 and p_1 channels, e.g., a $J^\pi=\frac{7}{2}^+$ resonance with $\Gamma_{p0}\ll\Gamma_{p1}$. Hence, when comparing their ^{22}Na$(n,p)^{22}$Ne results[1-3] to ^{19}F$(\alpha,p)^{22}$Ne data,[4] the authors of Refs. 1-3 looked for a resonance near the neutron threshold having $\Gamma_{p0}\ll\Gamma_{p1}$. Such a resonance does exist in the data of Ref. 4 at an energy of $E=0\pm4$ keV from the neutron threshold, having $\Gamma_{p0}/\Gamma_{p1}<0.03$. However, as noted in Ref. 3 the "strengths" given in Ref. 4 indicate that $\Gamma_\alpha\approx\Gamma_{p1}$, while the ^{22}Na + n measurements[1-3] indicate that $\Gamma_\alpha\ll\Gamma_{p1}$. Also, it was calculated in Ref. 1 that the parameters of this resonance in Ref. 4 lead to a width greater than the Wigner limit if $J^\pi=\frac{7}{2}^+$ is assumed, but the width for a $J^\pi=\frac{5}{2}^+$ assumption is below the limit. Furthermore, the width of the p_1 resonance observed by us and in Ref. 3 is probably too narrow to have been seen in the ^{19}F$(\alpha,p)^{22}$Ne measurements.[4,5] It is much more probable that the $\frac{5}{2}^+$ resonance we found to dominate the ^{22}Na$(n,p_0)^{22}$Ne cross section has been observed in the ^{19}F$(\alpha,p)^{22}$Ne measurements. In fact, a resonance has been observed[4] at $E=-6\pm4$ keV below the neutron

TABLE II. Comparison of resonance parameters determined in the present work to those from other measurements.

E_0	J^π	Widths or ratios of widths	Reaction	Reference
178 eV	$(\frac{7}{2})^+$	$\Gamma_n^0=2.7$ eV, $\Gamma_{p1}=148$ eV	^{22}Na(n,p)	Present work
		$\Gamma_{p0}/\Gamma_{p1}\ll 8.5\times10^{-3}$	^{22}Na(n,α)	
		$\Gamma_{\alpha0}/\Gamma_{p1}\ll 1.3\times10^{-3}$		
144 eV	$(\frac{7}{2})^+$	$\Gamma_n^0=2.8$ eV, $\Gamma_{p1}=114$ eV	^{22}Na(n,p)	3
		$\Gamma_{p0}/\Gamma_{p1}=6\times10^{-3}$		
		$\Gamma_{\alpha0}/\Gamma_{p1}\ll 1$		
<1 keV	$(\frac{7}{2})^+$	$\Gamma_{p0}/\Gamma_{p1}=7.4\times10^{-3}$	^{22}Na(n,p)	2
		$\Gamma_\alpha/\Gamma_p<2\times10^{-3}$		
	$(\frac{5}{2})^+$	$\Gamma_{\alpha0}/\Gamma_{p1}=(1\pm1.5)\times10^{-3}$	^{22}Na(n,p)	1
	$(\frac{5}{2})^+$	$\Gamma_{p0}/\Gamma_{p1}<1.0$,	^{22}Na(n,p)	Present work
		$\Gamma_{\alpha0}/\Gamma_{p0}=0.15$	^{22}Na(n,α)	
-11.2 keV		$\Gamma_{\alpha0}/\Gamma_{p0}=0.2$,[a] $\Gamma=2.2$ keV	^{19}F(α,p)	5
-10.5 keV[b]		$\Gamma_{p0}/\Gamma_{p1}>1.6\times10^{-3}$	^{22}Ne($p,p_1\gamma$)	5
		$\Gamma=1.4$ keV		
-5 keV		$\Gamma_{p0}/\Gamma_{p1}=0.3$,[c] $\Gamma<6$ keV	^{19}F(α,p)	4

[a]Given as $\Gamma_\alpha/\Gamma_{p1}$ in Ref. 5.
[b]Given as $+10.5$ keV in Ref. 5.
[c]Calculated from ratio of p_0 to p_1 "strengths," $(2J+1)\Gamma_\alpha\Gamma_p/\Gamma$, in Ref. 4.

threshold with $\Gamma_{p0}/\Gamma_{p1}=0.3$. This same resonance was also apparently observed in Ref. 5 although the resonance energy does not agree with that given in Ref. 4 to within the experimental errors, and there appear to be several mistakes in Ref. 5 which make it difficult to compare the results of Ref. 5 with other work.

Both Refs. 4 and 5 report two ^{19}F(α,p)^{22}Ne resonances near the neutron threshold. In both references it appears that the upper resonance is most strongly observed in the p_1 channel, while the lower resonance has a considerable p_0 strength as well. For these reasons it appears that the resonance observed in Ref. 4 at $E_\alpha=2354\pm4$ keV corresponds to the one in Ref. 5 at 2347.0 ± 0.5 keV and not the one in Ref. 5 at 2353.0 ± 0.5 keV. Instead, the resonance in Ref. 5 at 2353.0 ± 0.5 keV probably corresponds to the 2360 ± 4 keV resonance of Ref. 4. In other words, there is apparently an offset of about 7 keV in the energy calibration between the two experiments. The lower resonance was also apparently observed in Ref. 5 using the ^{22}Ne($p,p_1\gamma$)^{22}Ne reaction, although there appears to be a mistake in this reference regarding the position of the resonance with respect to the neutron threshold. This resonance is listed in Table II of Ref. 5 as being above the neutron threshold by 10.5 keV while the proton energy given and the discussion in Ref. 5 indicate that it is instead below threshold by this amount. Also, there appears to be a mistake in Ref. 5 regarding the ratio of widths for the $E_\alpha=2347$ keV resonance. Although the authors of Ref. 5 refer to this resonance as a "p_0 resonance" they give a ratio of the alpha width to the width for protons to the *first excited state,* $\Gamma_\alpha/\Gamma_{p1}=0.2$, for this resonance. Instead it appears that the ratio should be between the alpha width and the width for protons to the *ground state,* or $\Gamma_\alpha/\Gamma_{p0}=0.2$. If this is indeed the ratio that the authors of Ref. 5 meant to give, then it appears that this ^{19}F(α,p)^{22}Ne resonance is not only most likely the same resonance we observed in our p_0 measurements, but also could explain the α_0 cross section we measure at thermal energy. Using the ratio of our measured thermal cross sections implies, $\Gamma_{\alpha0}/\Gamma_{p0}=0.15$, in reasonable agreement with $\Gamma_\alpha/\Gamma_{p0}=0.2$ from Ref. 5. If this ^{19}F(α,p)^{22}Ne resonance is indeed the same one we see in our p_0 and α_0 measurements, the results of Refs. 5 and 6 indicate that it is probably too narrow to entirely account for our p_1 data above the region where the $\frac{7}{2}^+$ resonance fits our data. Instead, our higher-energy p_1 data probably show the results of one or more higher-energy resonances which we were not able to resolve in our measurements. Hence, the value $\Gamma_{p0}/\Gamma_{p1}=1.0$ we obtain for the $\frac{5}{2}^+$ resonance from the fits to our data can probably only be considered as an upper limit. This upper limit then is in agreement with the value $\Gamma_{p0}/\Gamma_{p1}=0.3$ obtained in Ref. 4 for their $E_\alpha=2354$ keV resonance.

Finally, the ^{19}F(α,n)^{22}Na and ^{22}Ne(p,n)^{22}Na data of Ref. 5 could in principal be converted using detailed balance and compared to our data. However, the data were apparently not corrected for a fairly large background and have not been corrected for the energy dependence of the detector efficiency which the authors indicate could cause as much as a 25% correction to the data. For these reasons, such a comparison is probably not worthwhile. To conclude this section, in an attempt to clarify the situation regarding ^{23}Na levels near the neutron threshold, we compare our results to previous work in Table II.

V. NUCLEOSYNTHESIS OF ^{22}Na

The ^{22}Na$(n,p)^{22}$Ne reaction may play the dominant role in the destruction of ^{22}Na in nucleosynthesis calculations where the neutron flux is substantial.[8–12] Hence, this reaction could have a significant impact on calculations of the possibility of observing ^{22}Na with gamma-ray telescopes.[7] Also, because ^{22}Ne is calculated to originate in some environments mainly from the decay of the ^{22}Na produced,[21] the ^{22}Na$(n,p)^{22}$Ne reaction may play a part in the explanation of the neon-E anomaly.[6]

We have calculated the astrophysical reaction rate $N_A\langle\sigma v\rangle$, for the ^{22}Na$(n,p)^{22}$Ne reactions ($p_0$ plus p_1) using our new data. The reaction rate to 0.3 GK was calculated using the fits to our data (solid curves in Figs. 2 and 3) and is shown in Fig. 5. To obtain the reaction rate at the highest temperatures shown in Fig. 5, the fits were extrapolated to energies higher than our measurements. The extrapolation is largest for the p_0 data. However, at all but the highest temperatures the rate is dominated by the p_1 channel and, hence, the large extrapolation in the p_0 channel probably has little effect on the total (n,p) reaction rate. The theoretical reaction rates[13,14] used in previous calculations are shown for comparison in Fig. 5. The theoretical rates range from about a factor of 10 too small at very low temperatures to about a factor of 5 too large at the highest temperatures measured. If this difference between the experimental and theoretical rates persists to higher temperatures, it may result in a significant change in the calculated production of ^{22}Na in explosive environments. For example, current estimates predict that approximately 3×10^{-5} solar masses of ^{22}Na is produced in a 25-solar-mass supernova explosion.[11,12] From this it has been calculated that explosions of galactic supernovae probably would be observable with an orbiting gamma-ray telescope.[7,11] The reduction in the ^{22}Na$(n,p)^{22}$Ne reaction rate indicated by our measurements makes an observation even more probable should such an event occur. Calculations employing the new, lower reaction rate which specifically address the production of ^{22}Na are needed to understand quantitatively the effect of this change in the rate on the likelihood of observing ^{22}Na with gamma-ray telescopes.

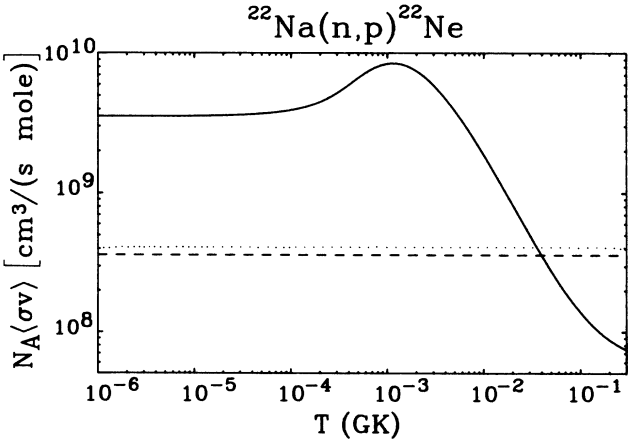

FIG. 5. Comparison of the ^{22}Na$(n,p)^{22}$Ne astrophysical reaction rate calculated from the sum of our p_0 plus p_1 data (solid curve), to the theoretical rates given in Refs. 13 (dashed curve) and 14 (dotted curve).

To be most useful in explosive nucleosynthesis calculations, the reaction rate is needed for temperatures higher than we currently can make measurements. This mainly is due to the fact that the proton storage ring (PSR) which drives the LANSCE white neutron source has so far run reliably at only about 24% of its design peak intensity. Perhaps when the PSR reaches design intensity, measurements can be extended to higher energies. In theory, the information necessary to extend the reaction rate to higher temperatures can be obtained by examining what has been learned about the structure of ^{23}Na near the neutron threshold using other reactions. In practice, very little is known about the structure of ^{23}Na in this region.[22] It appears that the most useful information comes from ^{19}F$(\alpha,n)^{22}$Ne measurements,[4] which reveal a resonance with $J=\frac{7}{2}$ at about 40 keV above the neutron threshold. It is possible that this resonance could contribute significantly to the ^{22}Na$(n,p)^{22}$Ne reaction rate at energies above our measurements, but within the range of interest in explosive nucleosynthesis calculations.

Finally, it should be noted that novae[21,23–26] may be significant sources of ^{22}Na. In novae, the ^{22}Na$(p,\gamma)^{23}$Mg reaction, whose rate has not been measured and hence is fairly uncertain,[27] is thought to be the dominant mechanism for destroying ^{22}Na, and neutrons do not appear to play a significant role.[21]

VI. CONCLUSIONS

Our measurements of the ^{22}Na$(n,p)^{22}$Ne and ^{22}Na$(n,\alpha)^{19}$F cross sections have revealed previously unknown information about the structure of ^{23}Na at energies near the neutron threshold. In contrast to previous studies[1–3] which assumed that a single resonance dominated both the p_0 and p_1 cross sections, our data reveal at least two resonances are need to explain both the p_0 and the p_1 data. Although it was conjectured in Ref. 5 that two resonances might be used to explain the available data, no firm conclusion could be drawn. On the other hand, our new data conclusively show that the p_1 cross section is dominated by a $(\frac{7}{2})^+$ resonance which contributes very little to the p_0 cross section. Instead, the p_0 and also most probably the (n,α_0) cross sections are dominated by a $(\frac{5}{2})^+$ resonance. We have shown that this latter resonance most probably corresponds to a level in ^{23}Na below the neutron threshold that has been observed in ^{19}F$(\alpha,p)^{22}$Ne (Refs. 4 and 5) and ^{22}Ne$(p,p_1\gamma)^{22}$Ne measurements.[5]

We have calculated the ^{22}Na$(n,p)^{22}$Ne astrophysical reaction rate using our new data and have shown that the theoretical rates[13,14] which have been used in previous nucleosynthesis calculations are approximately an order of magnitude different from the experimental one at most energies measured. This difference could have a significant impact on the calculated production of ^{22}Na and hence upon the likelihood of observing the ^{22}Na produced in a supernova explosion. This change in the reaction rate may also aid in the explanation of the neon-E anomaly[6] in meteorites.

ACKNOWLEDGMENTS

We wish to thank J. W. Starner for performing the gold-foil activation and for measuring the number of ^{22}Na nuclei in the samples for the OWR measurements. We gratefully acknowledge many helpful discussions with C. D. Bowman.

[1]R. Ehehalt, H. Morinaga, and Y. Shida, Z. Naturforsch. **26a**, 590 (1971).
[2]J. Kvitek, V. Hnatowicz, J. Cervena, J. Vacik, and V. M. Gledenov, Z. Phys. A **299**, 187 (1981).
[3]Yu. M. Gledenov, J. Kvitek, S. Marinova, Yu. P. Popov, J. Rigol, and V. I. Salatski, Z. Phys. A **308**, 57 (1982); Yu. M. Gledenov (private communication).
[4]J. Kuperus, Physica **31**, 1603 (1965).
[5]R. Ehelhalt, Y. Shida, C. Signorini, and H. Morinaga, Nuovo Cimento **15A**, 209 (1973).
[6]D. C. Black, Geochim. Cosmoschim. Acta **36**, 377 (1972).
[7]D. D. Clayton, Astrophys. J **198**, 151 (1975).
[8]W. D. Arnett, Astrophys. J **157**, 1369 (1969).
[9]W. M. Howard, W. D. Arnett, D. D. Clayton, and S. E. Woosley, Astrophys. J **175**, 201 (1972).
[10]J. W. Truran and A. G. W. Cameron, Astrophys. J **219**, 226 (1978).
[11]S. E. Woosley and T. A. Weaver, Astrophys. J **238**, 1017 (1980).
[12]S. E. Woosley and T. A. Weaver, in *Essays in Nuclear Astrophysics,* edited by C. A. Barnes, D. D. Clayton, and D. N. Schramm (Cambridge University Press, Cambridge, 1982), p. 377.
[13]R. V. Wagoner, Astrophys. J. Suppl. **18**, 247 (1969).
[14]S. E. Woosley, W. A. Fowler, J. A. Holmes, and B. A. Zimmerman, At. Data Nucl. Data Tables **22**, 371 (1978).
[15]P. E. Koehler, C. D. Bowman, F. J. Steinkruger, D. C. Moody, G. M. Hale, J. W. Starner, S. A. Wender, R. C. Haight, P. W. Lisowski, and W. L. Talbert, Phys. Rev. C **37**, 917 (1988).
[16]D. M. Chanley and W. R. Taylor (private communication).
[17]G. M. Hale, L. Stewart, and P. G. Young, Brookhaven National Laboratory Report BNL-NCS-51619, 1982, p. 25; G. M. Hale (private communication).
[18]V. Farinelli and M. Martini, Physica **29**, 1196 (1963).
[19]G. H. E. Sims, J. Inorg. Nucl. Chem. **29**, 593 (1967).
[20]R. D. Werner and D. C. Santry, J. Nucl. Energy **26**, 593 (1972).
[21]M. Arnould and H. Norgaard, Astron. Astrophys. **64**, 195 (1978).
[22]P. M. Endt and C. Van der Leun, Nucl. Phys. **A214**, 1 (1973).
[23]D. D. Clayton and F. Hoyle, Astrophys. J **187**, L101 (1974).
[24]R. K. Wallace and S. E. Woosley, Astrophys. J. Suppl. **45**, 389 (1981).
[25]W. Hillebrandt and F.-K. Thielemann, Astrophys. J. **255**, 617 (1982).
[26]M. Wiescher, J. Gorres, F.-K. Thielemann, and H. Ritter, Astron. Astrophys. **160**, 56 (1986).
[27]M. Wiescher and K. Langanke, Z. Phys. A **325**, 309 (1986).